Inorganic Chemistry
Article

Inorg. Chem. **2009**, *48*, 10405–10415 **10405**
DOI: 10.1021/ic9012334

Metal Loading Capacity of Aβ N-Terminus: a Combined Potentiometric and Spectroscopic Study of Zinc(II) Complexes with Aβ(1−16), Its Short or Mutated Peptide Fragments and Its Polyethylene Glycol−ylated Analogue

Chiara A. Damante,[†] Katalin Ősz,[‡] Zoltán Nagy,[§] Giuseppe Pappalardo,[∥] Giulia Grasso,[∥] Giuseppe Impellizzeri,[†] Enrico Rizzarelli,*[,†,∥] and Imre Sóvágó*[,§]

[†]*Department of Chemical Sciences, University of Catania, V. le A. Doria 6, 95125 Catania, Italy,* [‡]*Department of Physical Chemistry, University of Debrecen, 4010 Debrecen, Hungary,* [§]*Department of Inorganic and Analytical Chemistry, University of Debrecen, 4010 Debrecen, Hungary, and* [∥]*CNR Institute of Biostructures and Bioimaging, V. le A. Doria, 95125 Catania, Italy*

Received June 26, 2009

Aggregation of the amyloid β-peptide (Aβ) into insoluble fibrils is a key pathological event in Alzheimer's Disease (AD). There is now compelling evidence that metal binding to Aβ is involved in AD pathogenesis. The amino acid region 1-16 is widely considered as the metal binding domain of Aβ. In this work, we used a combined potentiometric, NMR, and electrospray ionization mass spectrometry (ESI-MS) approach to study the zinc(II) binding to a new polyethylene glycol (PEG)-conjugated peptide fragment encompassing the 1-16 amino acid sequence of Aβ (Aβ(1-16)PEG). Our results demonstrate for the first time that the Aβ(1-16) is able to coordinate up to three zinc ions, all the histidyl residues acting as independent anchor sites. The study was complemented by systematically investigating the zinc(II) complexes of a series of shorter peptide fragments related to the Aβ(1-16) sequence, namely, Aβ(1-4), Aβ(1-6), AcAβ(1-6), AcAβ(8-16)Y10A. The comparison of the whole results allowed the identification of the zinc(II) preferred binding sites within the longer Aβ(1-16) amino acid sequence. Unlike copper(II) that prefers the N-terminal amino group as the main binding site, the zinc(II) is preferentially placed in the 8-16 amino acidic region of Aβ(1-16).

Introduction

Alzheimer's disease (AD) is the main form of dementia occurring in the elderly. This disease is characterized by progressive loss of cholinergic neurons with concomitant damage of the cognitive function and memory.[1] The hallmark of AD is the formation of extracellular amyloid aggregates (senile plaques) and intracellular neurofibrillary tangles in the brain. The senile plaques mainly consist of a 39-43-residue peptide known as amyloid β (Aβ). Aβ is generated by the proteolytic action of β- and γ- secretases on the large transmembrane amyloid precursor protein (APP).[2,3] The amyloid cascade hypothesis proposes that an increased Aβ accumulation and aggregation into amyloid plaques is responsible of the neuronal dysfunction and, later on, of dementia.[4] Growing evidence is, however, pointing out that soluble Aβ oligomers, rather than the insoluble aggregated fibrils or protofibrils, cause the Aβ-mediated neurotoxic effects.[5−11] Environmental factors such as the pH, ionic strength, peptide concentration and temperature, metal ion levels[12,13] have been widely recognized as critical parameters

*To whom correspondence should be addressed. E-mail: erizzarelli@unict.it (E.R.), sovago@delfin.unideb.hu (I.S.). Phone: +39 095 7385070 (E.R.), +36 52 512900/22303 (I.S.). Fax: +39 095 337678 (E.R.), +36 52 489667 (I.S.).

(1) Arendt, T.; Bigl, V.; Tennstedt, A.; Arendt, A. *Neurosci. Lett.* **1984**, *48*, 81–85.
(2) Kuo, Y. M.; Emmerling, M. R.; Vigo-Pelfrey, C.; Kasunic, T. C.; Kirkpatric, J. B.; Murdoch, G. H.; Ball, M. J.; Rother, A. E. *J. Biol. Chem.* **1996**, *271*, 4077–4081.
(3) Checler, F. *J. Neurochem.* **1995**, *65*, 1431–1444.
(4) Hardy, J.; Selkoe, D. J. *Science* **2002**, *297*, 353–356.
(5) Cleary, J. P.; Walsh, D. M.; Hofmeister, J. J.; Shamkar, G. M.; Kuskowski, A. M.; Selkoe, D. J.; Ashe, K. H. *Nat. Neurosci.* **2005**, *8*, 79–84.
(6) Westerman, M. A.; Cooper-Blacketer, D.; Mariash, A.; Kotilinek, L.; Kawarabayashi, T.; Younkin, L. H.; Carlson, G. A.; Younkin, S. G.; Ashe, K. H. *J. Neurosci.* **2002**, *22*, 1858–1867.
(7) Selkoe, D. J. *Nat. Cell Biol.* **2004**, *6*, 1054–1061.
(8) Hoshi, M.; Sato, M.; Matsumoto, S.; Noguchi, A.; Yasutake, K.; Yoshida, N.; Sato, K. *Proc. Natl. Acad. Sci. U.S.A.* **2003**, *100*, 6370–6375.
(9) Lesnè, S.; Koh, M. T.; Kotilinek, L.; Kayed, R.; Glabe, C. G.; Yang, A.; Gallagher, M.; Ashe, K. H. *Nature* **2006**, *440*, 352–357.
(10) Walsh, D. M.; Klyubin, I.; Shankar, G. M.; Townsend, M.; Fadeeva, J. V.; Betts, V.; Podlisny, M. B.; Clary, J. P.; Ashe, K. H.; Rowan, M. J. *Biochem. Soc. Trans.* **2005**, *33*, 1087–1090.
(11) Garai, K.; Sahoo, B.; Kaushalya, S. K.; Desai, R.; Maiti, S. *Biochemistry* **2007**, *46*, 10655–10663.
(12) Snyder, S. W.; Ladror, U. S.; Wade, W. S.; Wang, G. T.; Barrett, L. W.; Matayoshi, E. D.; Huffaker, H. J.; Krafft, G. A.; Holzman, T. F. *Biophys. J.* **1994**, *67*, 1216–1228.
(13) Matsunaga, Y.; Saito, N.; Fujii, A.; Yokotani, J.; Takakura, T.; Nishimura, T.; Esaki, H.; Yamada, T. *Biochem. J.* **2002**, *361*, 547–556.

Published on Web 09/25/2009

affecting the conformation and the solubility of Aβ; more recently, based on the altered homeostasis of some transition metal ion in different brain compartments, the metal hypothesis of AD has been proposed to explain the origin of the pathology,[14] in contrast to the amyloid cascade hypothesis. In particular, it has been reported that copper(II) and zinc(II) ions play an important role in the aggregation of Aβ.[15−17] The amyloid peptide is precipitated by zinc(II) and copper(II) in vitro [18−21] and the concentration of these two metal ions is significantly elevated within AD plaques reaching values of 0.4 mM for copper(II) and 1 mM for zinc(II).[22] The role of these metal ions in amyloid fibrils formation has also been demonstrated by experiments showing that copper(II) and zinc(II) chelators are able to dissolve Aβ deposits in AD postmortem brains.[23,24] Furthermore, a deficiency of synaptic zinc(II) by the knockout of zinc transporters ZnT3 results in a reduced plaque formation in AD model mice, thus confirming the contribution of synaptic zinc(II) in the aggregation process.[25] The zinc(II) binding also influences the morphology of the Aβ aggregates, because zinc(II)-induced aggregates revealed to be more amorphous than those formed in the absence of this metal ion.[26−30]

Although it is well-established that zinc(II) can bind to Aβ, the effects of such a binding, in terms of metal-dependent aggregation and toxicity, are still controversial. At high concentration zinc(II) has been shown to promote Aβ-induced toxicity both in vitro [31] and in vivo.[32] By contrast, low levels of this metal ion reduced Aβ toxicity, thereby exerting a neuroprotective effect.[11,33−35] Thus it seems that zinc(II) may play a concentration-dependent role acting as an agent capable of turning Aβ's neurotoxicity on and off. Noteworthy is that such a dual effect could be also a function of the number of zinc(II) ions bound to Aβ. In fact, both the zinc(II) and Aβ are not equally distributed in the brain or in the whole central nervous system (CNS), the extracellular concentration of zinc(II) being very low in a large part of the brain areas.[36,37] By contrast, ionic zinc stored within the vesicles of certain glutamatergic neurons can reach millimolar concentrations. These zinc-enriched neurons are concentrated in selected areas of the brain, including the hippocampus, amygdale, and neocortex.[38] Therefore, the zinc(II)/Aβ ratio might be different from region to region.

It is now well-established that in the Aβ peptide, the metal-binding sites are located at the N-terminal hydrophilic region encompassing the amino acid residues 1-16 (Aβ(1-16)) whereas the C-terminal region, which contains hydrophobic amino acid residues, is not believed to be associated with any direct coordination of the metal ions.[39,40] The stoichiometry of the interactions of zinc(II) with Aβ is also elusive. In this regard complex stoichiometries from 1:1 [41] to 3:1 [42] have been proposed, suggesting the existence of multiple metal binding sites.

Different coordination environmnents have been proposed on the basis of several spectroscopic techniques including NMR,[40,43−46] Raman spectroscopy, circular dichroism, [41,47,48] or electrospray-ionization mass spectrometry (ESI-MS)[49]. In addition, the affinity constants until now reported are indicated as estimated, showing a large range of values.[50]

We have previously shown that the Aβ(1-16)PEG peptide derivative, obtained by attaching a polyethylene glycol (PEG) chain to the C-terminus of the Aβ(1-16) peptide fragment, is able to form very soluble multinuclear copper(II) complexes in aqueous solution.[51] This enabled a detailed potentiometric and spectroscopic characterization of the complex species, formed at different metal to ligand ratios by the Aβ(1-16)PEG-copper(II) system.

(14) Bush, A. I.; Tanzi, R. E. *Neurotherapeutics* **2008**, *5*, 421–432.
(15) (a) Suh, Y. H.; Checler, F. *Pharmacol. Rev.* **2002**, *54*, 469–525. (b) Multhaup, G.; Masters, C. L. *Met. Ions Biol. Syst.* **1999**, *36*, 365–387.
(16) Selkoe, D. J. *Physiol. Rev.* **2001**, *81*, 741–766.
(17) Bush, A. I. *Trends Neurosci.* **2003**, *26*, 207–214.
(18) Bush, A. I.; Pettingell, W. H., Jr.; Multhaup, G.; Paradis, M. D.; Vonsattel, J.-P.; Gusella, J. F.; Beyreuther, K.; Masters, C. L.; Tanzi, R. E. *Science* **1994**, *265*, 1464–1467.
(19) Bush, A. I.; Moir, R. D.; Rosenkranz, K. M.; Tanzi, R. E. *Science* **1995**, *268*, 1921–1923.
(20) Bush, A. I.; Pettingell, W. H., Jr.; Paradis, M. D.; Tanzi, R. E. *J. Biol. Chem.* **1994**, *269*, 12152–12158.
(21) Huang, X.; Atwood, C. S.; Moir, R. D.; Hartshorn, M. A.; Vonsattel, J.-P.; Tanzi, R. E.; Bush, A. I. *J. Biol. Chem.* **1997**, *272*, 26464–26470.
(22) Lovell, M. A.; Robertson, J. D.; Teesdale, W. J.; Campbell, J. L.; Markesbery, W. R. *J. Neurol. Sci.* **1998**, *158*, 47–52.
(23) Cherny, R. A.; Atwood, C. S.; Xilinas, M. E.; Gray, D. N.; Jones, W. D.; McLean, C. A.; Barnham, K. J.; Volitakis, I.; Fraser, F. W.; Kim, Y. S.; Huang, X.; Goldstein, L. E.; Moir, R. D.; Lim, J. T.; Beyreuther, K.; Zheng, H.; Tanzi, R. E.; Masters, C. L.; Bush, A. I. *Neuron* **2001**, *30*, 665–676.
(24) Cherny, R. A.; Legg, J. T.; McLean, C. A.; Fairlie, D. P.; Huang, X.; Atwood, C. S.; Beyreuther, K.; Tanzi, R. E.; Masters, C. L.; Bush, A. I. *J. Biol. Chem.* **1999**, *274*, 23223–23228.
(25) Lee, J. Y.; Cole, T. B.; Palmiter, R. D.; Suh, S. W.; Koh, J. Y. *Proc. Natl. Acad. Sci. U.S.A.* **2002**, *99*, 7705–7710.
(26) Yang, D. S.; McLaurin, J.; Qin, K.; Westaway, D.; Fraser, P. *Eur. J. Biochem.* **2000**, *267*, 6692–6698.
(27) Raman, B.; Ban, T.; Yamaguchi, K.; Sakai, M.; Kawai, T.; Naiki, H.; Goto, Y. *J. Biol. Chem.* **2005**, *280*, 16157–16162.
(28) Klung, G. M.; Losic, D.; Subasinghe, S. S.; Aguilar, M. I.; Martin, L. L.; Small, D. H. *Eur. J. Biochem.* **2003**, *270*, 4282–4293.
(29) Yoshiike, Y.; Tanemura, K.; Murayama, O.; Akagi, T.; Murayama, M.; Sato, S.; Sun, X.; Tanaka, N.; Takashima, A. *J. Biol. Chem.* **2001**, *276*, 32293–32299.
(30) House, E.; Collingwood, J.; Khan, A.; Korchazkina, O.; Berthon, G.; Exley, C. *J. Alzheimer's Dis.* **2004**, *6*, 291–301.
(31) Lovell, M. A.; Xie, C.; Markeshery, W. R. *Brain Res.* **1999**, *823*, 88–95.
(32) Bishop, G. M.; Robinson, S. R. *Brain Pathol.* **2004**, *14*, 448–452.
(33) Moreira, P.; Pereira, C.; Santos, M. S.; Oliveira, C. *Antioxid. Redox Signaling* **2000**, *2*, 317–325.
(34) Zhu, Y. J.; Lin, H.; Lal, R. *FASEB J.* **2000**, *14*, 1244–1254.
(35) Cuajungco, M. P.; Goldstein, L. E.; Nunomura, A.; Smith, M. A.; Lim, J. T.; Atwood, C. S.; Huang, X.; Farrag, Y. W.; Perry, G.; Bush, A. I. *J. Biol. Chem.* **2000**, *275*, 19439–19442.
(36) Frederickson, C. J.; Giblin, L. J.; Krezel, A.; et al. *Exp. Neurol.* **2006**, *198*, 285–293.
(37) Masuoka, J.; Saltman, P. *J. Biol. Chem.* **1994**, *269*, 25557–25561.
(38) Frederickson, C. J.; Bush, A. I. *Biometals* **2001**, *14*, 353–366.
(39) Kozin, S. A.; Zirah, S.; Rebuffat, S.; Hoa, G. H. B.; Debey, P. *Biochem. Biophys. Res. Commun.* **2001**, *285*, 959–964.
(40) Mekmouche, Y.; Coppel, Y.; Hochgrafe, K.; Guiloreau, L.; Talmard, C.; Mazarguil, H.; Faller, P. *ChemBioChem* **2005**, *6*, 1663–1671.
(41) Clements, A.; Allsop, D.; Walsh, D. M.; Williams, C. H. *J. Neurochem.* **1996**, *66*, 740–747.
(42) Atwood, C. S.; Scarpa, R. C.; Huang, X.; Moir, R. D.; Jones, W. D.; Fairlie, D. P.; Tanzi, R. E.; Bush, A. I. *J. Neurochem.* **2000**, *75*, 1219–1233.
(43) Syme, C. D.; Viles, J. H. *Biochim. Biophys. Acta* **2006**, *1764*, 246–256.
(44) Zirah, S.; Kozin, S. A.; Mazur, A. K.; Blond, A.; Cheminant, M.; Segales-Milazzo, I.; Debey, P.; Rebuffat, S. *J. Biol. Chem.* **2006**, *281*, 2151–2161.
(45) Lim, K. H.; Kim, Y. K.; Chang, Y. T. *Biochemistry* **2007**, *46*, 13523–13532.
(46) Danielsson, J.; Pierattelli, R.; Banci, L.; Gräslund, A. *FEBS J.* **2007**, *274*, 46–59.
(47) Liu, S. T.; Howlett, G.; Barrow, C. J. *Biochemistry* **1999**, *38*, 9373–9378.
(48) Suzuki, K.; Miura, T.; Takeuchi, H. *Biochem. Biophys. Res. Commun.* **2001**, *285*, 991–996.
(49) Zirah, S.; Rebuffat, S.; Kozin, S. A.; Debey, P.; Fournier, F.; Lesage, D.; Tabet, J.-C. *Int. J. Mass Spectrom.* **2003**, *228*, 999–1016.
(50) Faller, P.; Hureau„C. *Dalton Trans.* **2009**, 1080–1094.
(51) Damante, C. A.; Osz, K.; Nagy, Z.; Pappalardo, G.; Grasso, G.; Impellizzeri, G.; Rizzarelli, E.; Sóvágó, I. *Inorg. Chem.* **2008**, *47*, 9669–9683.

In this work we have employed a similar approach to examine the zinc(II) interaction with the Aβ(1-16)PEG peptide. Since a direct evaluation of the potentiometric data in the full-length Aβ(1-16)PEG would be complicated by the presence of several potentially zinc(II) binding residues (represented by the ^{6}His, ^{13}His, ^{14}His, ^{1}Asp, ^{7}Asp, ^{3}Glu, ^{11}Glu, ^{10}Tyr side chains in addition to the terminal amino group), we used an experimental approach consisting in the comparative study of a series of shorter peptide fragments, namely, the Aβ(1-4), Aβ(1-6), AcAβ(1-6), each one containing a potential zinc(II) binding site. The complexation properties of Aβ(1-16)Y10A and AcAβ(8-16)Y10A, in which ^{10}Tyr is replaced by an alanyl residue, were also studied to get information on a possible involvement of the phenolate group in zinc(II) coordination.

On the basis of a combined potentiometric and NMR procedure, we were able to (i) determine the different zinc(II) complex species as a function of the pH and the metal to peptide ratios in all the peptides investigated; (ii) determine the affinity constant values of the zinc(II) complexes with these peptides; and (iii) suggest a possible correlation between the coordination features of the different metal complexes determined in this paper, and the reported morphology of the various zinc-driven aggregates that show different toxicity.[31−35]

Experimental Section

General Procedures. All *N*-fluorenylmethoxycarbonyl (Fmoc)-protected amino acids, 2-(1-*H*-benzotriazole-1-yl)-1,1,3,3-tetramethyluronium tatrafluoroborate (TBTU), *O*-(*N*-Fmoc-2-aminoethyl)-*O*′-(2-carboxyethyl)-undecaethyleneglycol (PEG) and NovaSyn TGR resin were obtained from Novabiochem (Switzerland); Fmoc PAL-PEG resin, *N*,*N*-diisopropyl-ethylamine (DIEA), *N*-[(Dimethylamino)-1*H*-1,2,3-triazolo[4,5-b]-pyridine-1-ylmethylene]-*N*-methylmethanaminium hexafluorophosphate *N*-oxide (HATU), and 20% piperidine-DMF solution were obtained from Applied Biosystems. *N*-hydroxybenzotriazole (HOBt), triisopropylsilane (TIS), and trifluoroacetic acid (TFA) were purchased from Sigma/Aldrich. *N*,*N*-dimethylformamide (DMF, peptide synthesis grade) was obtained from Labscan Analytical Sciences.

All other chemicals were of the highest available grade and were used without further purification.

Preparative reversed-phase high performance liquid chromatography (RP-HPLC) was carried out using a Varian PrepStar 200 model SD-1 chromatography system equipped with a Prostar photodiode array detector with detection at 222 nm. Purification was carried out eluting with solvents A (0.1% TFA in water) and B (0.1% in acetonitrile) on a Vydac C18 250 × 22 mm (300 Å pore size, 10−15 μm particle size) column, at flow rate of 10 mL/min. Analytical RP-HPLC analyses were performed using a Waters 1525 instrument equipped with Waters 2996 photodiode array detector with detection at 222 nm. The peptide samples were analyzed using gradient elution with solvents A and B on a Vydac C18 250 × 4.6 mm (300 Å pore size, 5 μm particle size), run at flow rate of 1 mL/min.

Peptide Synthesis and Purification. Peptide synthesis and purification were described elsewhere.[51]

Potentiometric Measurements. The potentiometric titrations were performed in 3 cm^3 samples exploring the concentration range of 1×10^{-3} to 4×10^{-3} mol·dm^{-3} with metal ion to ligand ratios between 4:1 and 1:2. During the titration, argon was bubbled through the samples to ensure the absence of oxygen and carbon dioxide and also to stir the solutions. All measurements were carried out at 298 K and at a constant ionic strength of 0.2 mol·dm^{-3} KCl. pH measurements were made with a MOLSPIN pH-meter equipped with a 6.0234.100 combined electrode (Metrohm) and a MOL-ACS microburet controlled by a computer. The recorded pH values were converted into hydrogen ion concentration as described elsewhere.[52] Stability constants (log β_{pqr}) were calculated by means of the computational programs PSEQUAD,[53] SUPERQUAD, [54] and HYPERQUAD [55] by using eqs 1 and 2.

$$pM+qH+rL = M_pH_qL_r \quad (1)$$

$$\beta_{pqr} = [M_pH_qL_r]/[M]^p[H]^q[L]^r \quad (2)$$

Electrospray Ionization Mass Spectrometry (ESI-MS). ESI-MS spectra were recorded on a Finnigan LCQ Deca XP ion trap using an electrospray ionization (ESI) interface. Peptide solutions were introduced into the ESI source via a 100 μm i.d. fused silica, using a 500 μL syringe. The spectra were acquired in the positive ion mode, and the instrumental conditions were as follows: needle voltage 2.5 kV; flow rate 3−5 μL/min; source temperature 523−573 °C; m/z range 50−4000; cone potential 46 V; tube lens offset 15 V. The metal complex solutions were prepared by dissolving the peptide and $ZnSO_4$ (5×10^{-5} mol dm^{-3}) in Milli-Q water at 1:1, 1:2, and 1:3 L/Zn(II) ratios and were investigated in the 3−10.5 pH range, adjusting the pH values by adding HCl or NaOH.

Because of the isotopic distribution of elements, molecular species are detected in the mass spectra as clusters of peaks so that, to simplify their assignments, the m/z values indicated in the spectra and in the text correspond to the first (lowest-mass) peak of each cluster.

NMR Spectroscopy. All NMR spectra were acquired at 300 K on a Varian INOVA Unity-plus spectrometer operating at 499.884 MHz. Lyophilized samples of about 1×10^{-3}−2×10^{-3} mol dm^{-3} concentration were dissolved in 99.99% D_2O. Trimethylsilylpropionic acid (TSP) was used as an internal standard. The metal complex solutions were prepared by dissolving each peptide and $ZnCl_2$ in D_2O at metal ion to ligand ratio 1:1. The pH of the solutions was adjusted to pH 4.0, 5.0, 7.0 by adding the appropriate acid or base solution. The electrode-measured pH values were corrected for the isotope effect, according to the equation pD = pH + 0.4. Samples used to run ROESY experiments were prepared by dissolving the peptide in 90:10 H_2O/D_2O at a concentration of about 4×10^{-3} mol dm^{-3}. All the NMR measurements were carried out at a constant ionic strength of 0.2 mol·dm^{-3} KCl.

One-dimensional (1D) spectra were generally acquired with 8192 data points over a spectral width of 6000.2 Hz. Two-dimensional (2D) experiments were typically acquired with 2048 data points in the t2 dimension and 512 t1 increments. Water saturation was achieved by low power irradiation during the relaxation delay. TOCSY spectra were acquired with a spin locking field of 7 kHz at a mixing time of 70 or 80 ms. ROESY spectra were recorded using a 2 kHz spin locking field at a mixing time of 300 ms.

Results and Discussion

The protonation equilibria of the peptide fragments investigated in this study (Scheme 1) have been reported in a previous paper [51] where we demonstrated that PEG

(52) Irving, H.; Miles, G.; Malcolm, G.; Pettit, L. D. *Anal. Chim. Acta* **1967**, *38*, 475–488.

(53) Zékány, L.; Nagypál, I. In *Computational Methods for the Determination of Formation Constants*; Leggett, D. J., Ed.; Plenum Press: New York, 1985; pp 291−355.

(54) Gans, P.; Sabatini, A .; Vacca, A. *J. Chem. Soc., Dalton Trans.* **1985**, 1195–1200.

(55) Gans, P.; Sabatini, A .; Vacca, A. *Talanta* **1996**, *43*, 1739–1753.

Scheme 1. Amino Acid Sequences of the Peptide Fragments of Amyloid-β Polypeptide

Asp-Ala-Glu-Phe — **Aβ(1-4)**

Asp-Ala-Glu-Phe-Arg-His — **Aβ(1-6)**

Ac-Asp-Ala-Glu-Phe-Arg-His — **Ac-Aβ(1-6)**

Ac-Ser-Gly-Ala-Glu-Val-His-His-Gln-Lys — **Ac-Aβ(8-16)Y10A**

Asp-Ala-Glu-Phe-Arg-His-Asp-Ser-Gly-Ala-Glu-Val-His-His-Gln-Lys — **Aβ(1-16)Y10A**

Asp-Ala-Glu-Phe-Arg-His-Asp-Ser-Gly-Tyr-Glu-Val-His-His-Gln-Lys — **Aβ(1-16)**

Asp-Ala-Glu-Phe-Arg-His-Asp-Ser-Gly-Tyr-Glu-Val-His-His-Gln-Lys-PEG — **Aβ(1-16)PEG**

conjugation to Aβ(1-16) was useful to enhance the solubility of the resulting copper(II) complexes. As expected, the zinc(II) complexes with Aβ(1-16) revealed to be poorly soluble at nearly physiological pH even at 1:1 metal to ligand ratio.[44] Therefore the greater solubility of the Aβ(1-16)PEG-zinc(II) system allowed us to study the metal complexes in more detail exploring also different metal to ligand ratios.

Zinc(II) Complexes of the Peptides Aβ(1-4), AcAβ(1-6), and Aβ(1-6). The stability constant values of the complexes of Zn^{2+} with the tetrapeptide Aβ(1-4) and the hexapeptides AcAβ(1-6) and Aβ(1-6) are listed in Table 1. The simplest zinc(II) coordination mode was observed with the AcAβ(1-6) peptide ligand where metal coordination starts above pH 5 with the formation of the [ZnL] species. The stability constant value calculated for this complex species ($\log \beta = 2.55$) is slightly higher than that reported for the monodentate imidazole binding ($\log K = 2.15$ for acetyl-histamine, Ac-Hm),[56] indicating the additional binding of the carboxylate function of the glutamyl and/or aspartyl residues. A high molar fraction of uncomplexed metal ion is always present in the 5−12 pH range. This enables hydrolytic reactions to occur as the pH increases, and the precipitation of zinc(II)-hydroxide or mixed hydroxo complexes is observed above pH 8.

The Aβ(1-4) peptide can interact with the zinc(II) via the amino group and the carboxylate side chain of the aspartic acid at the N-terminus, forming a six-membered chelate ring. The stability constant value ($\log K = 3.73$) of the [ZnL] species (Table 1) is lower than the one reported for the similar complex species of β-alanine ($\log K_1 = 4.14$).[57]

This difference can be explained by considering the involvement of the carboxylate moiety belonging to the glutamate residue in zinc(II) coordination. The Glu carboxylate side chain can alternatively replace one of the aspartyl residues giving rise to a less stable complex species with the same (NH_2,COO^-) coordination mode, but forming a chelate ring of larger size. NMR experiments support this hypothesis. In fact, according to the potentiometric results, the zinc(II) does not perturb any resonance at pH 4 and 5, suggesting that the peptide ligand is predominately uncomplexed. At pH 7, where the [ZnL] species formation reaches its maximum, an upfield shift of the ^{1}Asp α-proton resonance is observed (see the NMR spectra of Aβ(1-4) in Supporting Information, Figure 1S). This is accompanied by changes of the coupling constant values $^3J_{\alpha,\beta}$ and $^3J_{\alpha,\beta'}$ pertinent to the ^{1}Asp residue ($^3J_{\alpha,\beta} = 5.0$ Hz and $^3J_{\alpha,\beta'} = 9.0$ Hz in the absence of zinc; $^3J_{\alpha,\beta} = 4.5$ Hz and $^3J_{\alpha,\beta'} = 6.7$ Hz in the presence of zinc). Taken together these results strongly suggest that the peptide binds to the metal ion through the amino and the carboxylate functions of the aspartyl residue. Interestingly the ^{3}Glu H_γ and $H_{\gamma'}$ resonances are also affected by the presence of zinc(II): a clear downfield shift of both signals is observed after zinc(II) addition (see in Supporting Information, Figure 2S). Furthermore the two multiplets get closer if compared to their chemical shift difference in the uncomplexed peptide. This evidence is also in agreement with the hypothesis of a partial involvement of the carboxylate function of ^{3}Glu in the coordination of the metal ion. Therefore, as already observed for the copper(II) complexes,[51] the zinc(II) binding to the peptide results in the formation of coordination isomers.

In the zinc(II)-Aβ(1-6) system, the formation of dinuclear complex species was evaluated by running the potentiometric titrations at 1:1 and 2:1 metal to ligand ratios. The results indicate the exclusive formation of mononuclear complexes without any evidence of dinuclear species. The species distribution diagram of the zinc(II)-Aβ(1-6) system (Figure 1) shows that the complexation of the metal ion starts at pH > 5 with the formation of the [ZnL] species.

In principle, both the N-terminal amino group and imidazole histidyl function may be the anchoring sites for the metal ion; the comparison of the stability constant value ($\log K = 4.32$) of the [ZnL] species with that

Table 1. Stability Constants of the Zinc(II) Complexes ($\log \beta_{pqr}$) with Aβ(1-6), Aβ(1-4), and AcAβ(1-6) Peptides ($T = 298$ K, $I = 0.2$ mol dm^{-3} KCl)[a]

Species	Aβ (1-4)	Aβ(1-6)	AcAβ(1-6)
[ZnL]	3.73(2)	4.32(1)	2.55(6)
[ZnH$_{-1}$L]		−4.05(2)	
[ZnH$_{-2}$L]		−12.96(2)	
pK(0/−1)		8.37	
pK(−1/−2)		8.91	

[a] pK(n/m) values reflect the pK values of zinc(II) complexes in the complex species.

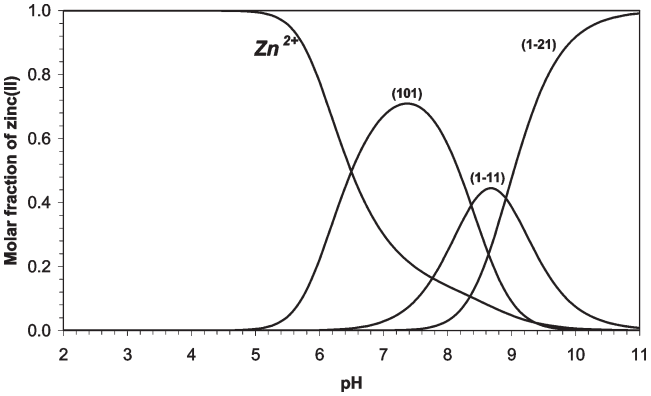

Figure 1. Species distribution diagram of the complexes formed in the zinc(II)−Aβ(1-6) system. ($c_{Zn(II)} = c_L = 2 \times 10^{-3}$ mol dm^{-3}).

(56) Kállay, C.; Ősz, K.; Dávid, A.; Valastyán, Z.; Malandrinos, G.; Hadjiliadis, N.; Sóvágó, I. *Dalton Trans.* **2007**, 4040–4047.
(57) Sóvágó, I.; Kiss, T.; Gergely, A. *Pure Appl. Chem.* **1993**, *65*, 1029–1080.

(log K = 3.73) found for the analogous zinc(II) complex with Aβ(1-4) indicates the formation of a macrochelate complex species in which both the amino and the imidazole nitrogens are involved in metal binding. The existence of such a macrochelate ring was already reported for the copper(II) complexes of Aβ(1-6).[51] A strong support of the macrochelate formation comes from NMR experiments, carried out at pH 7. Upon addition of zinc the ^{1}Asp α-proton resonance shifts toward upper field, as already observed for the zinc(II)-Aβ(1-4) system (Figure 2a).

At the same time, the signals associated with the C(2)H and C(5)H imidazole protons of ^{6}His broaden and appear down- and upfield shifted, respectively (Figure 2b). These selective spectral changes indicate that the zinc(II) is coordinated by the imidazole nitrogen and the N-terminal amino group. As expected, the $(CH_2)_\beta$ of ^{6}His and ^{1}Asp are affected by the coordination of the metal ion as well, but other important changes are observed in the aliphatic region. In particular, the broadening of the ^{3}Glu $(CH_2)\beta$ resonances and the shift of the Hγ and Hγ' signals of this residue, suggest that also the glutamyl side chain might be involved in zinc(II) coordination.

Thus, the [ZnL] species, which predominates at physiological pH, could be best described as a macrochelate with a (NH_2,N_{Im},COO^-) binding mode (Scheme 2a). In addition to the specific effects on the aspartyl, glutamyl, and histidyl residues, a detectable line-broadening and signal intensity reduction of several α-proton resonances is observed upon zinc(II) addition. This may originate from a chemical exchange rate between the uncomplexed and complexed peptide in an intermediate regime on the NMR time scale. Notably, not all the signals in the spectrum are affected to the same extent. This allows to rule out any eventual aggregation process.

A further increase of the pH leads to the formation of the complex species [$ZnH_{-1}L$] and [$ZnH_{-2}L$] with pK values of 8.37 and 8.91, respectively. These pK values can be equally attributed to hydroxo complex formation or to amide nitrogen deprotonation. It is difficult to distinguish between these two processes using potentiometry alone, so we resorted to ESI-MS experiments. Interestingly, the m/z values obtained for the [$ZnH_{-1}L$] and [$ZnH_{-2}L$] complex species (see Supporting Information, Table 1S) indicate that one and two deprotonated amide nitrogens, respectively, can take part in zinc(II) coordination.

Zinc(II) Complexes of the Peptide AcAβ(8-16)Y10A. AcAβ(8-16)Y10A can accommodate up to two zinc ions, and the stability constants of monuclear and dinuclear zinc(II) complexes are listed in Table 2.

The distribution curve diagram for the zinc(II)−AcAβ-(8-16)Y10A system at 1:1 metal to ligand ratio (Figure 3a) shows that the formation of the [ZnH_2L] species occurs at acidic pH values.

In this pH range, one imidazole nitrogen can act as the anchoring site for the metal ion. Moreover, the lysyl ammonium and one histidyl imidazole group are still protonated. In particular, the lysyl side chain is protonated until pH 10 suggesting that it cannot be included in the coordination of the metal ion. Taking into account the pK values of lysyl and histidyl side chains, we can calculate, for the [ZnH_2L], a log K = 2.88 which is higher than the stability constant expected for a monodentate

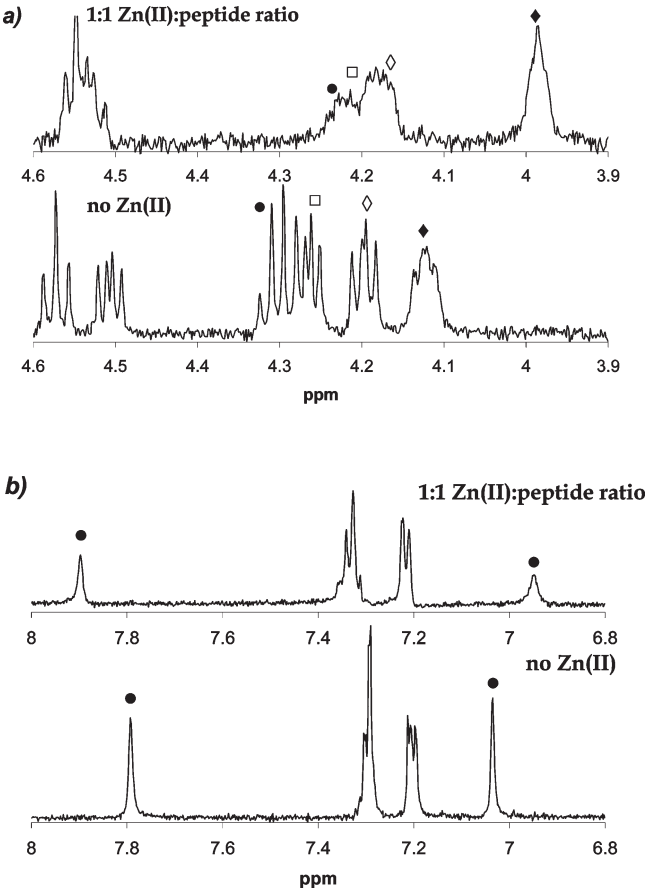

Figure 2. ^{1}H NMR spectra of Aβ(1-6) and zinc(II)−Aβ(1-6) system at 300 K, pH 7: (a) α-proton region (♦: ^{1}Asp, ◇: ^{3}Glu, □: ^{5}Arg, ●: ^{2}Ala), (b) aromatic proton region (●:C(2)H and C(5)H imidazole protons of ^{6}His). ($c_{Zn(II)} = c_L = 2 \times 10^{-3}$ mol dm^{-3} in 100% D_2O).

Table 2. Stability Constants of the Zinc(II) Complexes (log β_{pqr}) with AcAβ(8-16)Y10A Peptide (T = 298 K, I = 0.2 mol dm^{-3} KCl)[a]

mononuclear species		binuclear species	
species	log β	species	log β
[ZnH_2L]	19.92(1)	[$Zn_2H_{-2}L$]	−5.85(10)
[ZnHL]	13.94(1)	[$Zn_2H_{-3}L$]	−14.49(11)
[ZnL]	6.67(3)	[$Zn_2H_{-4}L$]	−25.65(11)
[$ZnH_{-1}L$]	−1.55(6)	pK(−2d/−3d)	8.64
[$ZnH_{-2}L$]	−11.20(6)	pK(−3d/−4d)	11.16
pK(2/1)	5.98		
pK(1/0)	7.27		
pK(0/−1)	8.22		
pK(−1/−2)	9.65		
pK(−2/−3)	11.45		

[a] pK(n/m) and pK(nd/md) values reflect the pK values of zinc(II) complexes in the mono- and binuclear species, respectively.

Zn(II)-imidazole species (log K = 2.15).[56] This indicates that the carboxylate group of ^{11}Glu may also assist the coordination of the metal ion forming a macrochelate with a (N_{Im},COO^-) binding mode. Again the NMR spectra are in line with this hypothesis. A significant and selective signal-broadening, together with a reduction in intensity of the α-proton resonances of ^{11}Glu and of one histidyl residue, are detected in the spectrum recorded at pH 5 after zinc(II) addition (Figure 4a). Unfortunately, the overlapping of the α-proton signals

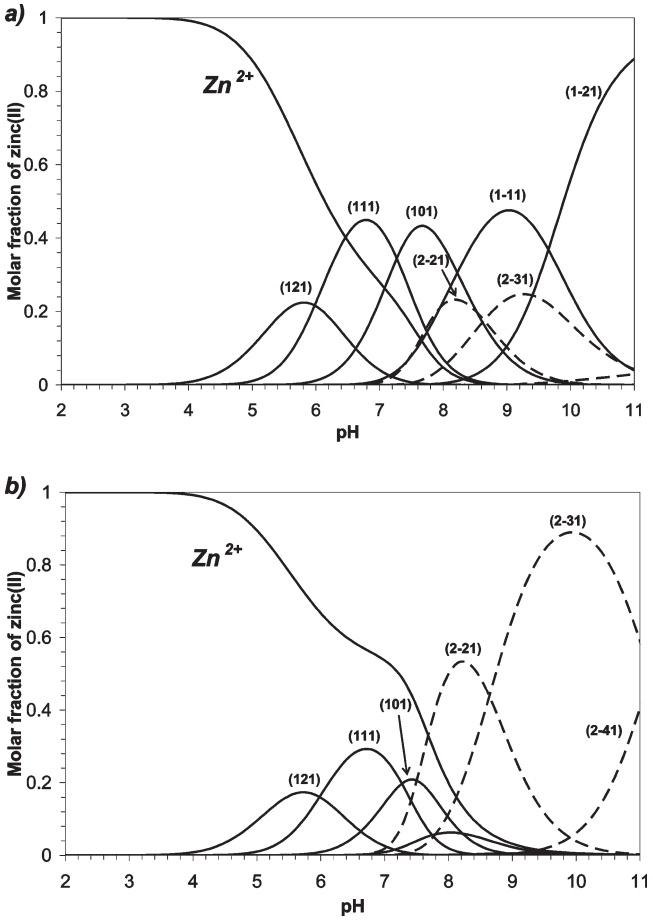

Figure 3. Species distribution diagram of the complexes formed in the zinc(II)−AcAβ(8-16)Y10A system. (a) $c_{Zn(II)} = c_L = 2 \times 10^{-3}$ mol dm^{-3}, (b) $c_{Zn(II)} = 4 \times 10^{-3}$ mol dm^{-3}, $c_L = 2 \times 10^{-3}$ mol dm^{-3}. Solid and dotted lined lines represent mono- and dinuclear species, respectively.

of the ^{13}His and ^{14}His residues prevents the univocal identification of the histidyl residue involved in the coordination.

Interestingly, the ^{12}Val protons are also affected by the metal ion (Figure 4b). In particular, both $(CH_3)_\gamma$ and $(CH_3)_{\gamma'}$ methyl resonances appear to be slightly shifted to higher field, and one of them is significantly broadened. Such an effect could be explained by considering the formation of the (N_{Im},COO^-) macrochelate which brings the zinc(II) close to the methyl groups of ^{12}Val, causing them to be perturbed. Similar spectral changes have been reported by other authors for the zinc(II) complexes of Aβ(Ac10-16) and Aβ(1-16).[43,44] It is important to note that, compared to the formation of zinc(II) complexes with Aβ(1-6) peptide, the coordination of the zinc(II) by AcAβ(8-16)Y10A starts at lower pH values. This means that, at least in acidic solution, the AcAβ(8-16)Y10A has an higher affinity for the zinc(II).

The deprotonation of the second histidyl imidazole group takes place above pH 5 (pK = 5.98). Considering the pK value of the protonated lysyl ammonium group, a log K = 3.63 can be obtained for the [ZnHL] complex species. Therefore, the deprotonation of the histidyl side chain increases the thermodynamic stability of this complex species thus supporting the hypothesis that this second imidazole ring enters in the coordination sphere of the zinc(II) which now results bound to the two

Scheme 2. Schematic Representation of the Possible Binding Modes of the Major Complex Species Formed in the Zinc(II)-Aβ(1-6) (a), Zinc(II)-AcAβ(8-16)Y10A (b), and Zinc(II)-Aβ(1-16)PEG (c) Systems[a]

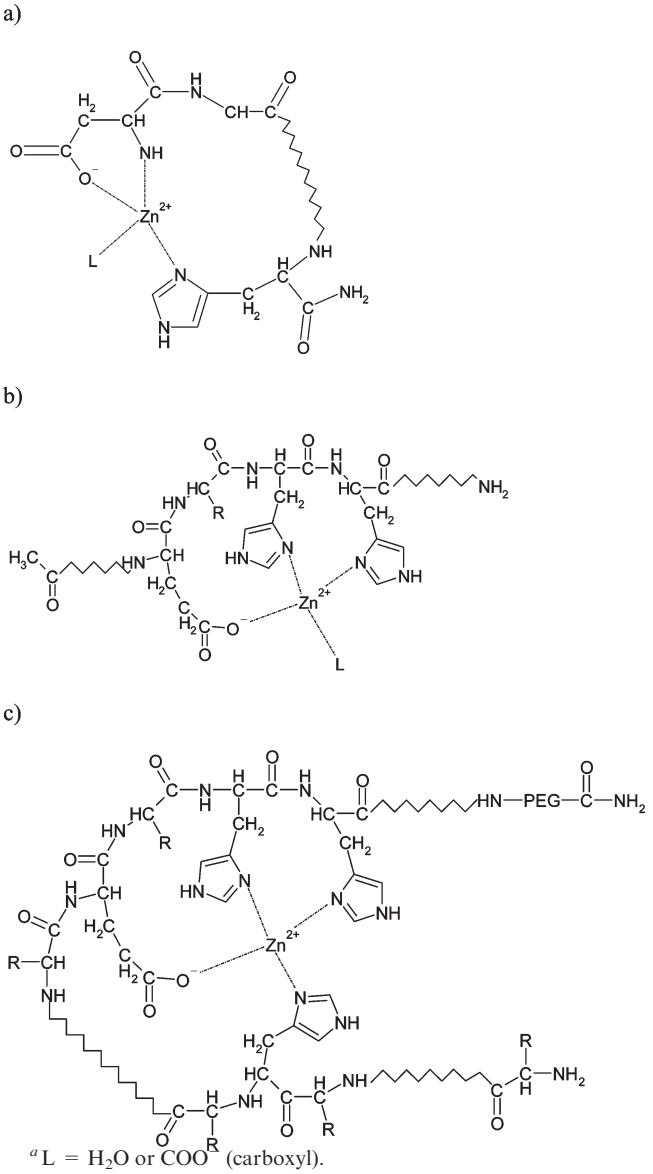

[a] L = H_2O or COO^- (carboxyl).

imidazole nitrogens and to the carboxylate group of ^{11}Glu forming a macrochelate with a ($2N_{Im}$,COO^-) binding mode (Scheme 2b). In agreement with this coordination mode, the aromatic protons of both ^{13}His and ^{14}His undergo a chemical shift variation and signal-broadening in the ^{1}H NMR spectrum carried out at pH 6.1 and in the presence of an equimolar amount of zinc-(II). The signals of the aromatic protons of the two histidyl residues completely disappear in neutral solution, where the [ZnHL] complex species reaches its maximum concentration (Figure 5).

The deprotonated [ZnL], [ZnH$_{-1}$L], and [ZnH$_{-2}$L] complex species, with the respective pK values of 7.27, 8.22, and 9.65, are formed at higher pH values. The last deprotonation reaction can be assigned to the amino group of the lysyl residue, while ESI-MS experiments permitted to distinguish between amide deprotonation and hydroxo complexes formation in the case of [ZnL] and [ZnH$_{-1}$L] complex species. Also in this case the m/z values of these complexes indicate

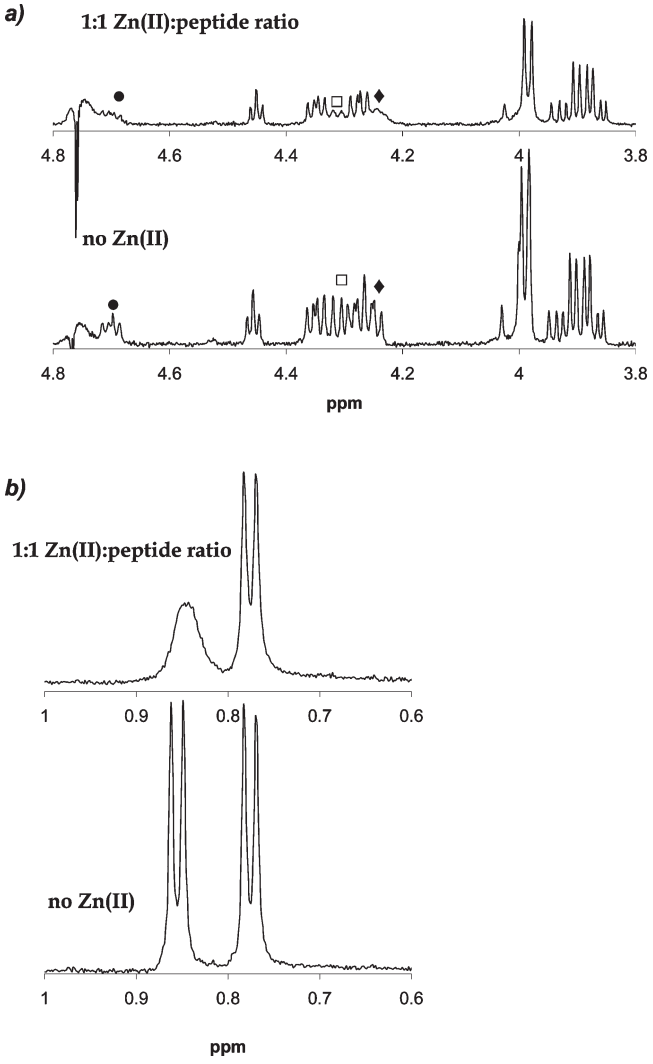

Figure 4. ^{1}H NMR spectra of AcAβ(8-16)Y10A and zinc(II)−AcAβ(8-16)Y10A system at 300 K, pH 5: (a) α-proton region (♦: ^{11}Glu, □: ^{10}Ala, ●: ^{13}His and ^{14}His), (b) ^{12}Val $(CH_3)_\gamma$ and $(CH_3)_{\gamma'}$ methyl resonances. ($c_{Zn(II)} = c_L = 2 \times 10^{-3}$ mol dm^{-3} in 100% D_2O).

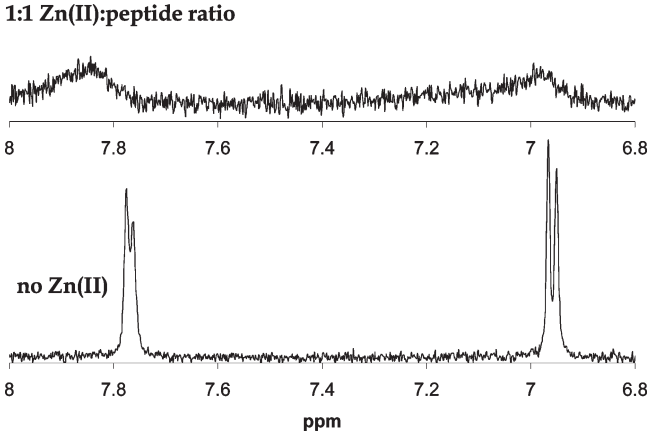

Figure 5. Aromatic region of ^{1}H NMR spectra of AcAβ(8-16)Y10A and zinc(II)−AcAβ(8-16)Y10A system at 300 K, pH 7. ($c_{Zn(II)} = c_L = 2 \times 10^{-3}$ mol dm^{-3} in 100% D_2O).

the presence of one and two deprotonated amide nitrogens in the coordination sphere of the zinc(II) (see the Supporting Information, Table 2S).

The potentiometric measurements revealed that the AcAβ(8-16)Y10A can host up to two zinc(II) ions forming dinuclear complex species. This further supports the evidence that this peptide fragment exhibits a higher affinity toward the zinc(II) in comparison with the Aβ(1-6). The formation of dinuclear complex species for AcAβ(8-16)Y10A was also confirmed by the ESI-MS experiments run in the presence of an excess of metal ion (see the Supporting Information, Table 2S).

The distribution curves diagram reported in Figure 3b shows that only 1:1 complexes are formed below pH 7. This observation represents an additional evidence of the involvement of both histidyl residues in the zinc(II) coordination in the mononuclear complex species [ZnHL] and [ZnL]. Binding of the second zinc(II) ion to the peptide occurs at pH $>$ 7, concomitantly with amide nitrogen deprotonation. As a consequence, each zinc(II) ion should be coordinated via one imidazole nitrogen and one or two additional amide functions. This hypothesis is confirmed by the ESI-MS results: the m/z value of the $[Zn_2H_{-1}L]$ species clearly indicates the presence of three deprotonated amide nitrogens in this complex species (see Supporting Information, Table 2S).

The high affinity of AcAβ(8-16)Y10A toward zinc(II) ions can probably be explained by the effect of the macrochelation via the two neighboring imidazole rings. Moreover, it is important to emphasize the role of the carboxylate function of the glutamyl residue, which contributes significantly to the chelation of the metal ion (Scheme 2).

Zinc(II) Complexes of the Peptide Aβ(1-16)PEG and Aβ(1-16)Y10A. The systematic analysis on the shorter peptide fragments Aβ(1-4), Aβ(1-6), AcAβ(1-6), and AcAβ(8-16)Y10A allowed us to know the coordination features of each separate metal binding site existing within the Aβ(1-16) amino acid sequence. The AcAβ(8-16)Y10A is able to bind up to two zinc(II) ions, while only mononuclear complexes are formed by the Aβ(1-6). The Aβ(1-16), that contains all the metal binding sites, is expected to bind as much as three zinc(II) ions. This is what we found by the potentiometric and ESI-MS measurements. The stability constant values of the zinc(II) complex species of Aβ(1-16)PEG are listed in Table 3.

To ascertain an active role of ^{10}Tyr in zinc(II) complexation, we also carried out potentiometric experiments on the Aβ(1-16)Y10A peptide and compared the results with those ones obtained for the wild type sequence.

Obviously Aβ(1-16)Y10A is expected to bind up to three zinc ions as well. However, because of the low solubility of the resulting trinuclear complexes, we were able to characterize only the zinc(II)-Aβ(1-16)Y10A complexes formed at 1:1 and 2:1 metal to ligand ratios (see the Supporting Information, Table 3S).

Because of the presence of the phenolate function of ^{10}Tyr, the Aβ(1-16)PEG has an additional protonation constant with respect to the Aβ(1-16)Y10A. Hence, from the point of view of the zinc(II) binding, the 1N complex with Aβ(1-16)PEG is the $[ZnH_5L]$ species while the analogue complex species of Aβ(1-16)Y10A is the $[ZnH_4L]$ species. Taking into account the protonation constant of the phenolate group of ^{10}Tyr, the stability constant values obtained for the zinc(II)-Aβ(1-16)PEG 1:1 and 2:1 systems are comparable with those obtained

Table 3. Stability Constants of the Zinc(II) Complexes (log β_{pqr}) with Aβ(1-16)PEG Peptide (T = 298 K, I = 0.2 mol dm^{-3} KCl)[a]

mononuclear species		binuclear species		trinuclear species	
species	log β	species	log β	species	log β
$[ZnH_7L]$	53.38(2)	$[Zn_2H_3L]$	35.35(6)	$[Zn_3L]$	17.87(9)
$[ZnH_6L]$	48.98(2)	$[Zn_2H_2L]$	29.47(1)	$[Zn_3H_{-1}L]$	10.19(6)
$[ZnH_5L]$	44.21(1)	$[Zn_2HL]$	22.44(2)	$[Zn_3H_{-2}L]$	2.60(2)
$[ZnH_4L]$	38.55(2)	$[Zn_2L]$	14.92(1)	$[Zn_3H_{-3}L]$	−6.07(1)
$[ZnH_3L]$	32.73(1)	$[Zn_2H_{-1}L]$	6.29(3)	$[Zn_3H_{-4}L]$	−15.43(2)
$[ZnH_2L]$	25.94(1)	$[Zn_2H_{-2}L]$	−3.02(5)	$[Zn_3H_{-5}L]$	−25.55(2)
[ZnHL]	17.66(2)	$[Zn_2H_{-3}L]$	−12.87(5)	$[Zn_3H_{-6}L]$	−36.20(4)
[ZnL]	8.92(3)	$[Zn_2H_{-4}L]$	−23.88(8)	$[Zn_3H_{-7}L]$	−47.65(8)
$[ZnH_{-1}L]$	−0.81(2)	$[Zn_2H_{-5}L]$	−35.74(9)	pK(0t/−1t)	7.68
$[ZnH_{-2}L]$	−11.30(3)	pK(3d/2d)	5.88	pK(−1t/−2t)	7.59
$[ZnH_{-3}L]$	−22.54(3)	pK(2d/1d)	7.03	pK(−2t/−3t)	8.67
pK(7/6)	4.40	pK(1d/0d)	7.52	pK(−3t/−4t)	9.36
pK(6/5)	4.77	pK(0d/−1d)	8.63	pK(−4t/−5t)	10.12
pK(5/4)	5.66	pK(−1d/−2d)	9.31	pK(−5t/−6t)	10.65
pK(4/3)	5.82	pK(−2d/−3d)	9.85	pK(−6t/−7t)	11.45
pK(3/2)	6.79	pK(−3d/−4d)	11.01		
pK(2/1)	8.28	pK(−4d/−5d)	11.86		
pK(1/0)	8.74				
pK(0/−1)	9.73				
pK(−1/−2)	10.49				
pK(−2/−3)	11.24				

[a] pK(n/m) values reflect the pK values of zinc(II) complexes.

for the corresponding complex species of Aβ(1-16)Y10A, thereby indicating that the absence of ^{10}Tyr does not change the coordination properties of this peptide fragment. This means that the phenolate group of tyrosine is not involved in the coordination of the zinc(II) and that both peptide fragments have the same zinc(II) binding mode. Thus, from now on, we will refer only to the metal complexes of Aβ(1-16)PEG.

The species distribution diagram of the zinc(II)-Aβ(1-16)PEG system is reported in Figure 6. It shows the formation of both mononuclear and dinuclear complex species, with the mononuclear species predominating in the slightly acidic pH range.

As reported above, AcAβ(8-16)Y10A binds to zinc(II) more efficiently than Aβ(1-6) in the slightly acidic pH range. Thus, the two neighboring histidyl residues are expected to be the primary metal binding sites in the whole Aβ(1-16) peptide ligand. To prove it, 1D and 2D ^{1}H NMR experiments were carried out on Aβ(1-16) both in the absence and in the presence of equimolar zinc(II) at pH 5. The use of the 2D-NMR techniques allowed the assignment of the resonances of the three histidyl and two glutamyl residues.

The addition of the metal ion was accompanied by a slight upfield shift of the $(CH_3)_\gamma$ methyl resonances of ^{12}Val together with a significant broadening of one of the two doublet (Figure 7a). An identical effect on ^{12}Val was observed also for the Zn(II)-AcAβ(8-16)Y10A 1:1 system and, in that case, was attributed to the formation of a macrochelate species with a (N_{Im},COO^-) binding mode. This result confirms that the zinc(II) is preferentially placed in the 8-16 amino acidic region of Aβ(1-16).

The signals of the amide protons of ^{12}Val, ^{13}His, ^{14}His, and ^{11}Glu are selectively reduced in intensity and broadened in the presence of zinc(II) (Figure 7b) indicating that, in the acidic pH range, the zinc(II) is coordinated in a macrochelate complex species through the imidazole

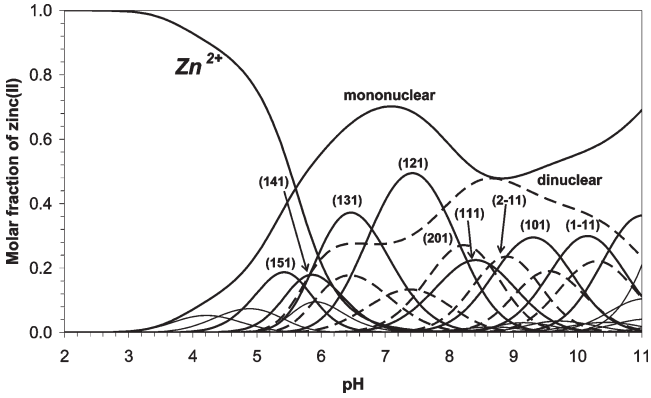

Figure 6. Species distribution diagram of the complexes formed in the zinc(II)−Aβ(1-16)PEG system ($c_{Zn(II)}$ = c_L = 2 × 10^{-3} mol dm^{-3}). Solid and dotted lines represent mono- and dinuclear species, respectively.

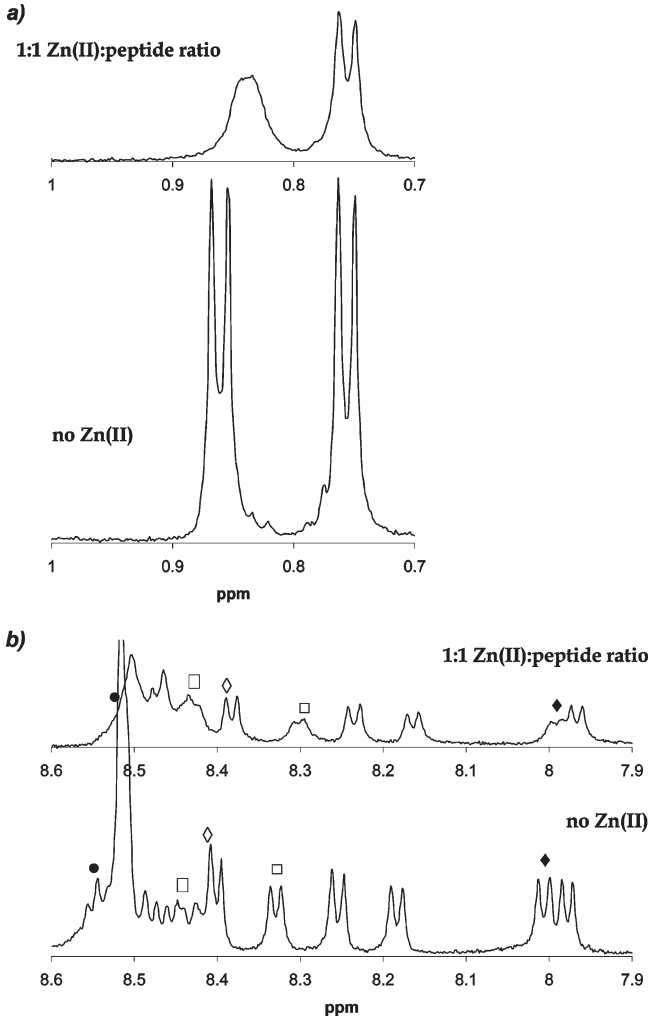

Figure 7. ^{1}H NMR spectra of Aβ(1-16) and zinc(II)−Aβ(1-16) system at 300 K, pH 5: (a) ^{12}Val $(CH_3)_\gamma$ and $(CH_3)_{\gamma'}$ methyl resonances, (b) amide proton region (♦: ^{12}Val, □: ^{11}Glu, ◇: ^{13}His, □: ^{14}His and ●: ^{6}His). ($c_{Zn(II)}$ = c_L = 4 × 10^{-3} mol dm^{-3} in 90% H_2O + 10% D_2O).

nitrogens of ^{13}His or ^{14}His in addition to the carboxylate group of ^{11}Glu. Further support to this coordination mode is obtained by the value of the stability constant for the chelation of one His nitrogen and the ^{11}Glu carboxylate, calculated taking into account the pK values of the protonated residues (the lysyl, tyrosyl, aspartyl

amino groups and the imidazole nitrogens of two histidyl residues). The log $K = 3.18$ value, obtained for the species $[ZnH_5L]$, is similar to that found for the analogue zinc(II) complex species with AcAβ(8-16)Y10A peptide fragment, confirming the (N_{Im},COO^-) binding mode proposed above for the $[ZnH_5L]$ complex species. However, in the case of the Aβ(1-16)PEG, the possibility to form several coordination isomers, with the same (N_{Im},COO^-) binding mode, slightly increases the stability of this $[ZnH_5L]$ species.

The deprotonation of a second histidyl residue occurs by increasing the pH (pK = 5.66). A stability constant value log $K = 3.91$ can be calculated for the resulting $[ZnH_4L]$ complex species. The deprotonation reaction is accompanied by an increase of the thermodynamic stability of the complex species, indicating that a second imidazole nitrogen is involved in the coordination sphere of the zinc(II) in addition to the first histidyl and glutamyl residues forming a macrochelate with ($2N_{Im}$,COO^-) binding mode. Such a result is in line with that found for the zinc(II)-AcAβ(8-16)Y10A system. This unambiguously establishes that in the acidic pH range the zinc(II) is preferentially bound to the 8-16 amino acid region of Aβ(1-16), through the ^{13}His/^{14}His dyad and the ^{11}Glu carboxylate side chain.

A further increase of the pH value leads to the formation of the $[ZnH_3L]$ and $[ZnH_2L]$ complex species. In the $[ZnH_3L]$ species the N-terminal amino group, the tyrosine and lysine side chains are still protonated. The $[ZnH_2L]$ is the major species in the physiological pH range and, unlike the $[ZnH_3L]$ species, the N-terminal amino group is now deprotonated. Therefore, in the $[ZnH_2L]$ species, the N-terminal amino group and the three histidyl residues can be considered as potential binding sites, thereby increasing the chance to form coordination isomers. The stability constant value of the $[ZnH_3L]$ complex (log K = 4.82) is significantly higher than that (log $K = 3.63$) found for the analogues [ZnHL] complex species formed with AcAβ(8-16)Y10A, in which a ($2N_{Im}$,COO^-) coordination mode is proposed. This difference indicates the involvement of the third His residue in zinc(II) coordination. Figure 8 shows the 1H-NMR spectra recorded at pH 7, of Aβ(1-16)PEG and the changes induced by the addition of zinc(II) on the aromatic group resonances.

The ^{13}His and ^{14}His aromatic protons signals almost disappear upon zinc(II) addition (Figure 8). These selective changes prove that, in neutral solution, the metal ion is bound to the ^{13}His/^{14}His dyad, and that the carboxylate groups participate in metal coordination. The imidazole signals of ^{6}His are also perturbed by the zinc(II) (Figure 8). The C(2)H and C(5)H protons are broadened and respectively downer and upper-field shifted, suggesting that the imidazole side chain of this amino acid residue might be also involved in the metal ion coordination (see Scheme 2c).

The further increase of the stability constant value of $[ZnH_2L]$ species (log $K = 5.72$) in the zinc(II)-Aβ(1-16)PEG system, may suggest the involvement of the N-terminal amino group.

In the ^{1}H NMR spectrum recorded at pH 7, the ^{1}Asp α-proton resonance is upfield shifted by -0.023 ppm (Figure 9). However this upfield shift is much less significant than the one detected in the case of zinc(II)-Aβ(1-6) system ($\Delta\delta = -0.138$ ppm) in which the coordination through the N-terminal group is assumed.

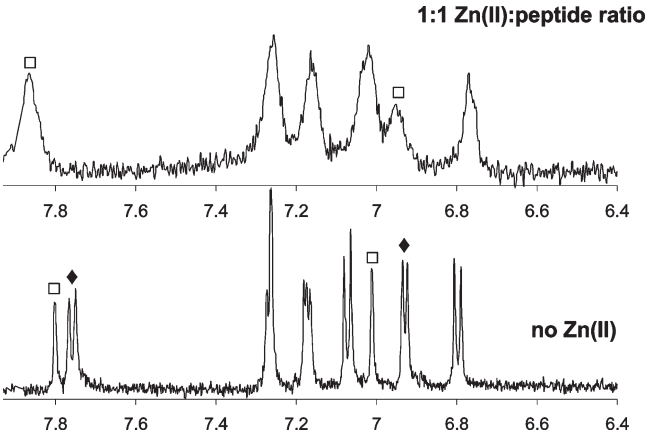

Figure 8. Aromatic region of ^{1}H NMR spectra of Aβ(1-16)PEG and zinc(II)−Aβ(1-16)PEG system at 300 K, pH 7 (♦: ^{13}His and ^{14}His, □: ^{6}His). ($c_{Zn(II)} = c_L = 2 \times 10^{-3}$ mol dm^{-3} in 100% D_2O).

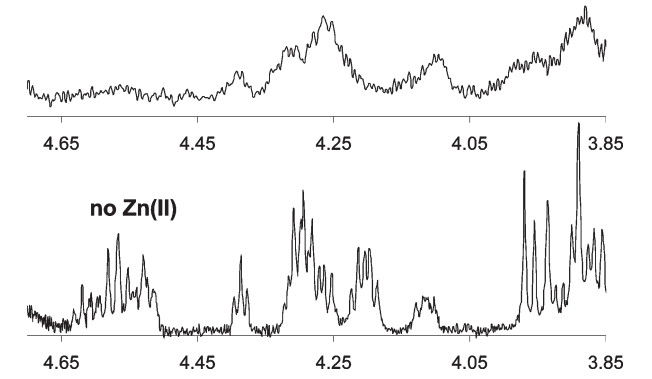

Figure 9. CH_α region of ^{1}H NMR spectra of Aβ(1-16)PEG and zinc-(II)−Aβ(1-16)PEG system at 300 K, pH 7. ($c_{Zn(II)} = c_L = 2 \times 10^{-3}$ mol dm^{-3} in 100% D_2O).

To ascertain an eventual involvement of the amino group in the binding to zinc(II) ion, NMR experiments were carried out also at pH 7.5 both in the absence and in the presence of 0.5 mol equiv of zinc(II) to increase the percentage of the $[ZnH_2L]$ species over the $[ZnH_3L]$ one (see distribution diagram in the Supporting Information, Figure 3S). Unfortunately, at this pH value the presence of zinc(II) caused evident line broadening of almost the totality of the resonances. However, from the residual crosspeak of the ^{1}Asp α-proton detected in the 2D-COSY spectrum, only a small variation of the chemical shift was observed upon zinc(II) addition. This would indicate no significant involvement of the N-terminal amino group in the metal ion coordination. At the same time, on the basis of the potentiometric result it cannot be ruled out that, above pH 7, the zinc(II) might be distributed among different binding sites, namely, the ^{13}His/^{14}His dyad and the N-terminal amino group, with a definite preference for the former site.

Interestingly, Figure 6 shows the existence of binuclear complex species even at 1:1 metal to ligand ratio. In this complex species both the 1-6 and 8-16 domains of Aβ(1-16)PEG bind a zinc(II) ion. The existence of

dinuclear and even trinuclear species (see distribution diagrams in the Supporting Information, Figures 3S and 4S) was also confirmed by the ESI-MS experiments carried out in the presence of an excess of metal ion (see the Supporting Information, Table 4S). Noteworthy, our ESI-MS results are in agreement with a recent study on the interaction of the Aβ(1-40) with pairs of metal ions in which it is clearly indicated that more than one zinc ion can bind to Aβ (1-40) and the majority of the observed complex species in the ESI-MS spectra belong to monomolecular Aβ complexes with more than one ion of zinc.[58]

The dissociation constants of the zinc(II)-Aβ complexes reported in the literature show different values owing to the variety of experimental conditions and techniques used. It has been reported that Aβ(1-40) binds a zinc(II) ion with high affinity (K_d = 100 nmol/L) and two additional zinc(II) ions with somewhat lower affinity (K_d = 5 μmol/L).[20] However, successive results showed the formation of only 1:1 complex with K_d = 3.2 μmol/L.[41] Similar values in the low micromolar range (i.e., 5−10 μM) have also been reported for truncated Aβ(1-16)[40] and for Aβ(1-28)[46]. Yet, different results were obtained by other authors despite the similar experimental conditions used. Ricchelli et al. found a K_d in the low micromolar range for Aβ(1-16), Aβ(1-40), and Aβ(1-42) [59] whereas Garson et al. deduced a higher K_d of 300 μM for Aβ(1-40) and 57 μM for Aβ(1-42) [60]. As mentioned above the different methodologies and experimental conditions used may explain the variability in the reported values. More recently the great variability of affinity constant values has been attributed both to the aggregation state of the peptide ligands and to the use of different buffers such as Tris, HEPES, or PBS, which can compete with Aβ for the binding of the metal ion.[50,60] It is noteworthy that the reported stability constant values were indicated as (i) estimated, (ii) comprised in a range, and (iii) related to a binding site and not to a specific metal complex species.[20,40,41,46,50,59−62]

NMR measurements have been carried out to discriminate among the different coordination environments experienced by zinc(II) in the various complex species formed with Aβ.[40,43−46,62,63] There is a general consensus indicating the involvement of the three histidyl residues, ^{6}His, ^{13}His, ^{14}His, [40,43−49] while the identity of further ligands remains controversial. The involvement of ^{11}Glu and ^{1}Asp has been proposed by some authors,[40,43,45,46,62] while others exclude the binding of the ^{1}Asp.[44] A comparison between the different experimental conditions of the NMR experiments, that is, pH values, and the speciation obtained on the basis of our thermodynamic investigation can explain these contrasting results. In fact, the [ZnH_2L] species, in which the N-terminal amino group is deprotonated and then able to coordinate the zinc(II), is almost the only complex species existing around pH 7.4 and at ligand to metal ratio higher than two (see distribution diagram in the Supporting Information, Figure 5S). By contrast the data obtained below pH 7 refer to a mixture of two mononuclear complexes [ZnH_3L] and [ZnH_2L] and various dinuclear species (see Figure 6). This means that the NMR data obtained below pH 7 cannot be attributed to a single complex species. This fact prevents the unambiguous assignments of the donor atoms involved in each complex species.

Conclusion

According to the amyloid cascade hypothesis,[4] the deposition of Aβ diffuse plaques is a critical event that may be associated with AD pathogenesis. Metal ions, particularly zinc(II), had been proposed to play a significant role in the assembly and neurotoxicity of Aβ-aggregates in AD.[11,17] Studies on the zinc(II)-Aβ interactions suggested that this metal had a major effect on Aβ aggregation either increasing the aggregation at high zinc concentration or reducing the aggregation at low metal ion concentration.[17,21,64,65] A key parameter in the Aβ-zinc(II) interaction is the affinity of the peptide ligand for the metal ion. In this regard the need to obtain reliable thermodynamic data has recently stressed.[50,61]

In the present paper, the first potentiometric study of the zinc(II) complexes with the N-terminal region of Aβ enabled us to determine the stability constants of zinc(II) complexes and the true affinity of this metal ion toward the soluble and monomeric Aβ peptide. Such a study also demonstrates that Aβ is able to allocate up to 3 equiv of zinc(II) ion, a result that is in line with that of Bush et al.[20] In addition our results show which species form at different metal to ligand ratios and pH values, thereby contributing to answer the question of the formation and survival of different zinc(II) complexes with Aβ in different brain areas, where different concentration values of both Aβ and zinc(II) can occur.[50] Our potentiometric data indicate that the stoichiometry of the main complexes formed at physiological pH changes as a function of the metal to peptide ratios. In other words the mononuclear [ZnH_2L], dinuclear [Zn_2HL], and trinuclear [Zn_3L] species predominate at physiological pH at 1:1, 2:1, and 3:1 M/L, respectively (Figure 6 and see distribution diagrams in the Supporting Information, Figures 4S and 5S). Considering that the zinc(II) concentration in the brain is higher than that one of Aβ, the formation of polynuclear zinc complexes, in physiological conditions, may be not an improbable process. Recently, it has been suggested that the zinc(II)-binding affinity to the full-length Aβ is rather independent of the aggregation state of the polypeptide chain.[66]

The systematic study of zinc(II) complexes with the shorter Aβ fragments was useful not only to map up all the potential zinc sites within the whole Aβ(1-16), but also to identify the preferential binding sites of the zinc(II) ions. In particular, the comparison of the stability constant values of the zinc(II)

(58) Drochioiu, G.; Manea, M.; Dragusanu, M.; Murariu, M.; Dragan, E. S.; Petre, B. A.; Mezo, G.; Przybylski, M. *Biophys. Chem.* **2009**, *144*, 9–20.
(59) Ricchelli, F.; Drago, D.; Filippi, B.; Tognon, G.; Zatta, P. *Cell. Mol. Life Sci.* **2005**, *62*, 1724–1733.
(60) Garzon-Rodriguez, W.; Yatsimirsky, A. K.; Glabe, C. G. *Bioorg. Med. Chem. Lett.* **1999**, *9*, 2243–2248.
(61) Tongu, V.; Karafin, A.; Palumaa, P. *J. Neurochem.* **2008**, *104*, 1249–1259.
(62) Gaggelli, E.; Janicka-Klos, A.; Jankowska, E.; Kozlowski, H.; Migliorini, C.; Molteni, E.; Valensin, D.; Valensin, G.; Wieczerzak, E. *J. Phys. Chem. B* **2008**, *112*, 100–109.
(63) Curtain, C. C.; Ali, F.; Volitakis, I.; Cherny, R. A.; Norton, R. S.; Beyreuther, K.; Barrow, C. J.; Masters, C. L.; Bush, A. I.; Burnham, K. J. *J. Biol. Chem.* **2001**, *276*, 20466–20473.
(64) Garai, K.; Sengupta, P.; Sahoo, B.; Maiti, S. *Biochem. Biophys. Res. Commun.* **2006**, *345*, 210–215.
(65) Cardoso, S. M.; Rego, A. C.; Pereira, C.; Oliveira, C. R. *Neurotox. Res.* **2005**, *7*, 273–281.
(66) Talmard, C.; Bouzan, A.; Faller, P. *Biochemistry* **2007**, *46*, 13658–13666.

complexes with both the N-terminus and the C-terminus fragments of Aβ(1-16), clearly shows the preference of zinc(II) to bind to the His domain of the C-terminus. This preference is different from that found for the copper(II) ion that forms more stable complexes with the N-terminus domain.[51]

Such an apparent difference might have biological consequences in terms of Aβ's aggregation morphology and toxicity. Both inhibitory and fibril-inducing activities have been reported for Cu^{2+}[48,67−69] and Zn^{2+} [11,18,26−30], respectively. It has been reported that the aggregation of Aβ in the presence of zinc(II) or copper(II) is very different. Unlike copper(II), zinc(II) is able to strongly induce Aβ aggregation. However, zinc(II) induced Aβ aggregates revealed to be more amorphous than the fibrillar observed in the presence of copper(II); the different morphology and toxicity of the aggregates depend on the concentration and metal to peptide ratios.[11,32,33,70] Our previous[51] and present results establish that the N-terminal region of Aβ can give access to different Cu^{2+} and Zn^{2+} coordination environments that change under slightly different experimental conditions. Thus, it is very likely that the different metal complex species can lead to profound changes in Aβ self-assembly, morphology, and neurotoxicity.

Acknowledgment. This work was supported by MIUR, FIRB RBNE03PX83, and FIRB RBIN04L28Y (E.R.), the MTA(Hungary)-CNR(Italy) bilateral program and OTKA 77586 (Hungary). The authors thank Mrs. Tiziana Campagna for technical assistance.

Supporting Information Available: Additional information as noted in the text. This material is available free of charge via the Internet at http://pubs.acs.org.

(67) Atwood, C. S.; Moir, R. D.; Huang, X. D.; Scarpa, R. C.; Bacarra, N. M. E.; Romano, D. M.; Hartshorn, M. K.; Tanzi, R. E.; Bush, A. I. *J. Biol. Chem.* **1998**, *273*, 12817–12826.
(68) Zou, J.; Kajita, K; Sugimoto, N. *Angew. Chem., Int. Ed.* **2001**, *40*, 2274–2277.
(69) Karr, J. W.; Szalai, V. A. *Biochemistry* **2008**, *47*, 5006–5016.
(70) Noy, D.; Solomonov, I.; Sinkevich, O.; Arad, T.; Kjaer, K.; Sagi, I. *J. Am. Chem. Soc.* **2008**, *130*, 1376–1383.